Journal of Physics and Chemistry of Solids 91 (2016) 158–162

Contents lists available at ScienceDirect

Journal of Physics and Chemistry of Solids

journal homepage: www.elsevier.com/locate/jpcs

Effects of high-temperature annealing on ESR properties of solid solutions of garnet minerals

T.K. Gundu Rao [a], Nilo F. Cano [b,*], Jose F.D. Chubaci [a], S. Watanabe [a]

[a] Instituto de Física, Universidade de São Paulo, Rua do Matão, Travessa R, 187, São Paulo, CEP 05508-090 SP, Brazil
[b] Departamento de Ciências do Mar, Universidade Federal de São Paulo, Santos, SP, Brazil

ARTICLE INFO

Article history:
Received 11 October 2015
Received in revised form
23 December 2015
Accepted 6 January 2016
Available online 7 January 2016

Keywords:
ESR
TL
F^+-center
Garnets
High-temperature annealing

ABSTRACT

A garnet (G7) silicate mineral belonging to pyralspite subgroup was studied using the technique of electron spin resonance (ESR). This study shows that iron is present in G7 as isolated species as well as species coupled by dipolar interactions. The ESR data shows a gradual increase of cluster of Fe^{3+} ions accompanied by decrease of dipolar interactions and increase of possible exchange interactions at high temperature. The $Fe^{2+} \rightarrow Fe^{3+}$ oxidation process occurs in the garnets as a function of annealing temperature. Thermoluminescence (TL) peaks at approximately 190 and 340 °C are observed in the irradiated G7 garnet. Investigations using the technique of ESR were carried out to identify the centers involved in the TL process.

1. Introduction

Six silicate minerals are components of the Garnet Group. They are almandine, pyrope, spessartine, grossular, andradite and uvarovite, the three first belonging to a subgroup of the name pyralspite and the three other to the subgroup called ugrandite [1]. Each one of them are end garnet that is very seldom found in nature. What one finds in the nature is a solid solution, large part of garnets of pyralspite subgroup. The general chemical formula of the pyralspite garnets is $X_3Al_2Si_3O_{12}$ and since grossular has formula $Ca_3Al_2Si_3O_{12}$ very often grossular participate in the solid solution [1]. Almandine is the variety that is found abundantly, therefore, in large number of solid solution almandine is present. Whenever in a solid solution one component appear with more than 90%, it is considered a garnet with that component.

Watanabe et al. [2] investigated two solid solutions of pyralspite garnets, one called G3 which contains almandine (54.89%) and spessartine (43.94%) in almost equal percentage, and the other called G4 which predominantly almandine and pyrope in solution. G3 presented an absorption spectrum with about 12 absorption bands in UV, visible and near infrared region, in this last one bands at 1270 nm and 1600 nm are attributed to Fe^{2+}. Annealing G3 sample at 900 to 1100 °C these bands are reduced due to $Fe^{2+} \rightarrow e^- + Fe^{3+}$ reaction. The ESR spectrum of a natural G3 sample consists of a straight line extending from 1000 to 6000 Gauss magnetic field with an elevated slope. Annealing at above 900 °C that straight line changes into a typical signal at $g=2.0$ due to Fe^{3+}. This signal becomes very large for further annealing at 1000–1100 °C. This is due to the fact that at this temperature the conversion of Fe^{2+} into Fe^{3+} increases the intensity of the signal at $g=2.0$.

Neves et al. [3] investigated two solid solutions of pyralspite garnets, one called G5 with 79.51% almandine, 11.71% pyrope, 4.50% spessartine and 4.27% grossular, the other one named G6 with 86.09% almandine (almost pure), 4.007% pyrope and 8.709% grossular. The optical absorption spectra of G5 and G6 are similar to that of G3 sample. The Fe^{2+} band at 1270 and 1600 nm under high temperature annealing change into Fe^{3+} ion like in G3 sample, while Fe^{2+} band in G5 does not change. Since in G6 a large fraction of iron is found in Fe^{2+} state, its ESR spectrum is practically without signal, but after annealing at temperature higher than 800 °C due to change of Fe^{2+} into Fe^{3+} signal due to this ion at $g=2.0$ is observed. G5, on the other hand, has shown an unexpected ESR behavior. The natural sample presented a spectrum with a signal with $g=9.0$, which changes to a signal with $g=6.0$ after 800 °C annealing. At 900 °C annealing the signal moves to $g=3.2$ and for higher temperature annealing again a typical $g=2.0$ signal due to Fe^{3+} ions is observed. Ikeya [4] has shown that magnetite, Fe_3O_4, shows $g=9.0$ signal, hematite. Fe_2O_3, $g=6.0$ signal and the limonite, a signal at $g=3.2$. Thus, it seems that iron in G5 forms magnetite, hematite, limonite molecules

* Corresponding author.
E-mail addresses: nilocano@if.usp.br, nilo.cano@unifesp.br (N.F. Cano).

http://dx.doi.org/10.1016/j.jpcs.2016.01.004
0022-3697/

depending on the annealing temperature.

The objective of the present work is to study the nature of paramagnetic centers and luminescence in a new solid solutions of garnet, labeled as G7, measuring the effects of high-temperature annealing and gamma irradiation through electron spin resonance (ESR) and thermoluminescence (TL) techniques. An attempt has been made to understand the magnetic and luminescence properties which depend on the defects and magnetic ions in this mineral.

2. Experimental details

The new sample of garnet (G7) investigated here was obtained at the town of Governador Valadares, State of Minas Gerais, Brazil. These samples were crushed and sieved to retain grains 0.080–0.180 mm in size for TL and ESR measurements, while grains smaller than 0.080 mm in diameter were used in the X-rays fluorescence (XRF) and X-ray diffraction analysis that were performed the Geology Department of University of São Paulo.

The XRF analysis indicated this sample is actually a solid solution with 64.15% almandine, 23.84% pyrope and 6.33%. spessartine.

A Bruker EMX ESR spectrometer operating at X-band frequency with 100 kHz modulation frequency was utilized for ESR experiments. The *g*-factors of defect centers were calibrated using Diphenyl Picryl Hydrazyl (DPPH) as a standard sample. Temperature dependence of the ESR spectra was studied using a Bruker BVT 2000 variable temperature accessory. The TL measurements were performed in a nitrogen atmosphere using a model 4500 Harshaw TL reader equipped with two photomultiplier tubes, which could record luminescence signals independently. The reader was controlled by WinREMS Software, which was supplied with the spectrometer and was run on a Windows computer. The heating rate used in the TL measurements was 4 °C/s. Each point in the glow curve represents an average of five readings. A calibrated ^{60}Co source was used for irradiating the samples to gamma rays.

3. Results and discussion

The room temperature ESR spectrum of G7 is shown in Fig. 1(a). The spectrum exhibits signals at $g\sim4.3$ and 7.9. As the major constituent of the present garnet system is almandine, it is likely that the observed signals are due to Fe ions. There is a minor contribution from spesartine and as Mn is part of the spesartine garnet, ESR from Mn^{2+} ions is expected in the room temperature spectrum. However, there is no clear indication of the characteristic six line spectrum from Mn^{2+} ions in the observed spectrum. The ESR lines with different *g*-values are indication of the presence of iron in different symmetry environments.

Iron can exists in several valence states viz., Fe^{+}, Fe^{2+}, Fe^{3+} and Fe^{4+} [5]. In general, the most common forms are Fe^{2+} and Fe^{3+}. Fe^{3+} ions exhibit ESR spectra at room temperature while Fe^{2+} with an electronic configuration $3d^6$ is observable at very low temperatures (<5 K) due to short relaxation time at room temperature. The electronic configuration of Fe^{3+} ions is [Ar] $3d^5$ and the spin quantum number is 5/2 and the ground state is $^6S_{5/2}$. With the orbital angular momentum $L=0$ in crystals, a crystalline electric field alone can't split an S state. Higher order perturbations involving spin–orbit coupling and spin–spin coupling lead to splitting. In this situation, ESR spectrum of Fe^{3+} ions is characterized by lines which depend on the local symmetry of Fe^{3+}

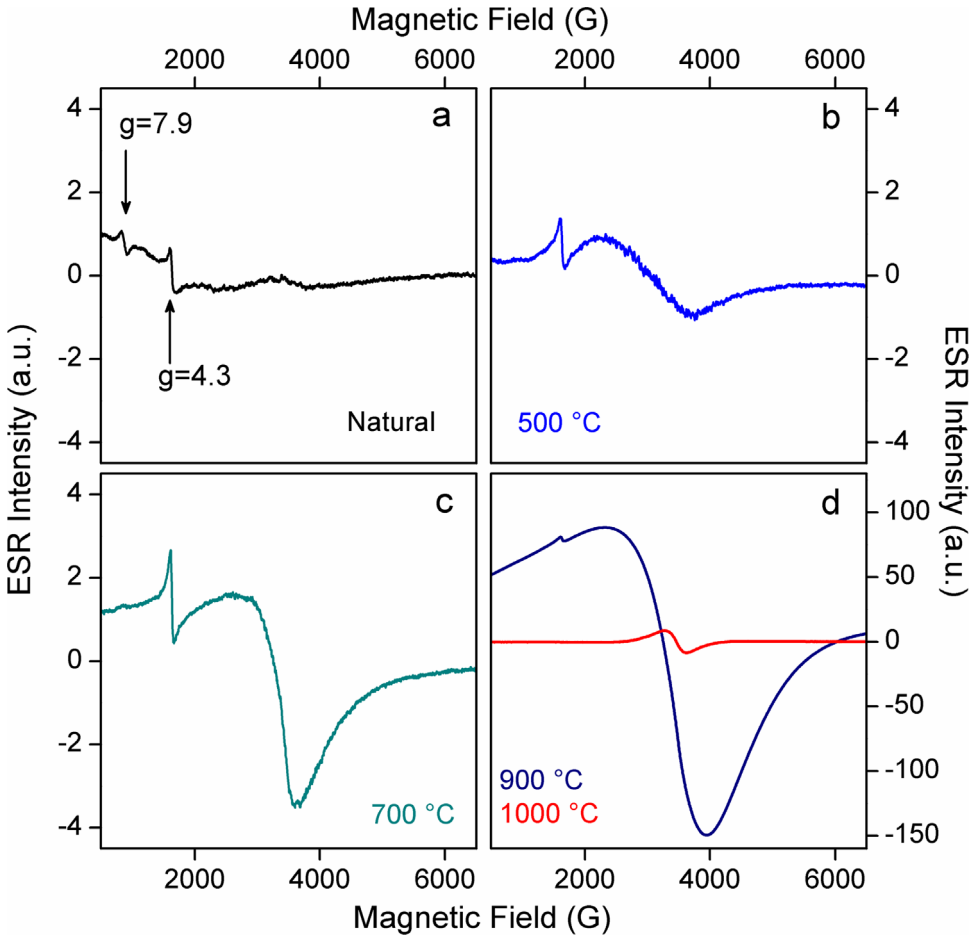

Fig. 1. ESR spectrum at room temperature of G7 system: (a) natural, (b) annealed at 500 °C, (c) annealed at 700 °C, (d) annealed at 900 °C and 1000 °C.

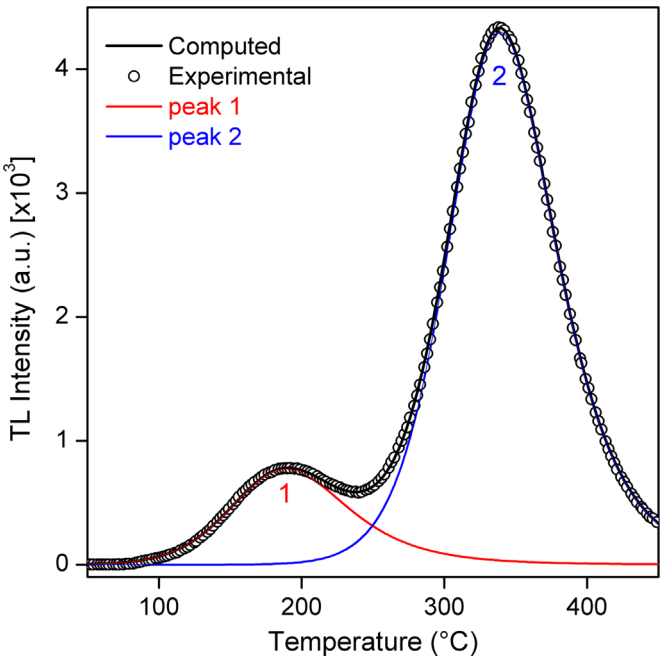

Fig. 2. TL glow curve of natural G7 pre-annealed at 500 °C and subsequently receiving a gamma-ray dose of 10 kGy. A good fit between the experimental glow curve (circles) and the simulated glow curve (full line) can be achieved by assuming the presence of two TL peaks at 190 °C (red line) and 340 °C (blue line). (For interpretation of the references to color in this figure legend, the reader is referred to the web version of this article.)

ions and the magnitude of crystal field interactions.

Fe^{3+} ions with a ground state with $L=0$ is expected to give rise to an ESR line at $\sim g=2.0$. In a study of Fe doped glass system, Costner et al. [6] have shown by theoretical considerations that Fe^{3+} ion in a distorted environment displays lines in the low field region specifically in their case at $g \approx 4.38$ and $g \approx 8.6$. Several authors have also carried out theoretical analysis of Fe^{3+} ion in different symmetry surroundings and different magnitudes of crystal field interaction. In particular, Brodbeck [7] has shown that the orthorhombic nature of the crystal field is given by $E/D=\lambda$ and a purely rhombic field results when the ratio $\lambda=0.33$ while $E/D=0$ corresponds to a crystal field of axial symmetry. D and E are the second-order crystal field terms with axial and rhombic symmetry respectively. It was suggested that a single ESR line with $g_{eff}=4.27$ will be observed when the microwave energy ($h\nu$) is much smaller than the axial distortion term D. Consequently, the observed ESR line at $g=4.3$ in the present garnet system arises from an Fe^{3+} ion subjected to a relatively strong crystal field and located at a low symmetry environment.

Fig. 1(b) shows the ESR spectrum of a G7 which has been annealed at 500 °C. Apart from the line at $g=4.3$, a new low intensity broad line with a linewidth of about 1440 gauss and a resonance field of 3050 gauss is observed. This indicates that the isolated Fe^{3+} species are still present in the annealed sample and a coupled Fe^{3+} species begins to appear as a low field broad line. The large linewidth arises from dipolar interactions between Fe^{3+} ions which seem to be present as a cluster in the garnet system. The internal dipolar fields in the cluster results in the appearance of the ESR line at low magnetic fields. As almandine contribution is quite high in the garnet solid solution, there exists considerable concentration of Fe ions. The ESR lines are of low intensity in the natural sample and as such all the Fe ions at the eight-fold coordinated sites in almandine are in the Fe^{2+} state. It is speculated that the new broad line seen at low fields in the 500 °C annealed garnet are due to $Fe^{2+} \rightarrow Fe^{3+}$ oxidation process. It is to be noted that the resonance absorption at $g \sim 7.9$ is not seen in the annealed sample.

The ESR spectrum from the 700 °C annealed sample is shown in Fig. 1(c). Three features can be noticed in the spectrum. Isolated Fe^{2+} ions are still present and there is an increase in the intensity of clustered Fe^{3+} ions which points to an increased conversion of Fe^{2+} ions to Fe^{3+} ions at high temperatures. The linewidth has decreased ($\sim$930 Gauss) and the broad line has shifted towards high field (resonance field $\sim$3300 Gauss). These are indicative of reduction of dipolar interactions resulting in reduction of linewidth and also dipolar internal fields. This trend continues at 900 °C anneal (linewidth $\sim$540 Gauss) and the observed ESR spectrum is shown in Fig. 1(d). Considerable changes, however, are seen in the 1000 °C annealed G7 system (Fig. 1(d)). ESR line is now seen near $g \sim 2$ region and there is a large increase in the concentration of Fe^{3+} ions which points to an efficient $Fe^{2+} \rightarrow Fe^{3+}$ conversion at this temperature. Further, there is a drastic reduction in the linewidth ($\sim$360 Gauss). This feature indicates that the clustered Fe^{3+} species are now coupled by exchange interactions and dipolar interactions are negligible. It is well known that exchange interactions lead to line narrowing effects. It is inferred from the annealing studies that the predominant interaction at low annealing temperatures is dipolar interaction while at high temperatures the exchange interactions dominate. The crystal structure of almandine with Fe^{2+}–O–Fe^{2+}–O–Fe^{2+} networks is well suited for dipolar fields to be present at each Fe^{3+} ion. Further with increasing in concentration of Fe^{3+} ions, there is also a high probability for exchange interactions to occur as evidenced by present experimental findings.

The G7 system exhibits a TL glow peak at approximately 190 and 340 °C after gamma irradiation with 10 kGy. The glow curve is shown in Fig. 2. The glow curves for the samples were obtained at a heating rate of 4 °C/s. Applying the CGCD equations proposed by Kitis et al. [8] we obtain the deconvolution of TL glow curve of G7. The deconvolution analysis has shown the TL glow curve of the G7 crystal is composed of two peaks of second order kinetic in the region between 100 and 450 °C (see Fig. 2).

Defect centers are induced in the G7 after gamma irradiation and the resulting room temperature ESR spectrum after irradiation is shown in Fig. 3. Thermal annealing experiments at different high

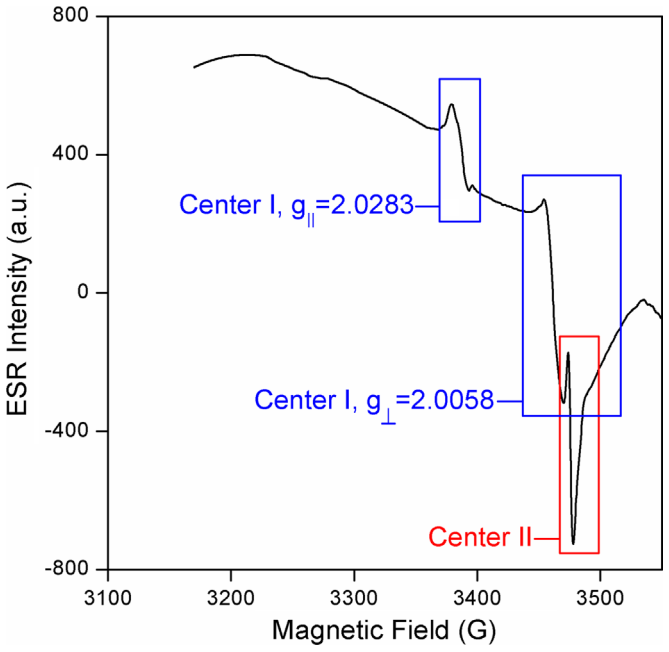

Fig. 3. Room temperature ESR spectrum of irradiated G7 (gamma dose: 20 kGy). Line labeled as I is due to an O_2^- ion. Center II line is assigned to a F^+ center.

temperatures point to the presence of two defect centers. The ESR lines associated with these centers are labeled in Fig. 3.

Among the rock-forming silicates, almandine, $Fe_3^{2+}Al_2Si_3O_{12}$, is an important class of garnet mineral and is the ferrous end member of this group of silicates. Like other garnets, almandine silicate crystallizes in the cubic space group *Ia3d* with unit cell parameter $a=11.51$ Å [9] and 160 atoms in the unit cell. The structure consists of Fe^{2+} cations located at a site coordinated to eight oxygens in a dodecahedral arrangement. Al^{3+} ions occupy six-fold coordinated octahedral sites along with Si^{4+} ions at sites with tetrahedral coordination with four oxygens [9,10]. Every pair of Fe^{2+} ions is connected by two identical pathways formed by oxygen bridges with a Fe–O–Fe angle of 101°.

In almandine crystal lattice, antisite cation exchange is probable wherein Al atoms will partially replace Fe sites. Such replacements, called as cation exchange disorder, is a point defect in crystal lattices involving exchange of cation positions. Kuklja [11], based on theoretical calculations, has predicted the occurrence of such defects. X-ray diffraction [12], X-ray absorption fine structure [13] and direct observation by high-angle annular dark-field (HAADF) and annual bright-field scanning transmission electron microscopy [14] have confirmed their presence in crystals. Several trapping sites for the electron and hole on irradiation are created due to antisite formation which results from the interchange of the ions in the octahedral and dodecahedral positions by divalent and trivalent ions.

The line labeled as center I in Fig. 3 does not exhibits any hyperfine splitting and the center is characterized by an axially symmetric g-tensor with principal values $g_{\|}=2.0283$ and $g_{\perp}=2.0058$. Gamma irradiation normally leads to the formation of V-centers, F-centers and F^+-centers (an electron trapped at an anion vacancy) in oxide systems [15]. Apart from these centers, superoxide O_2^- ion is also known to form in oxides particularly on their surfaces. One way for the formation of O_2^- ion is a direct transfer of an electron from the oxide surface to an adsorbed oxygen molecule. An alternate pathway in oxide systems has been suggested by Garrone et al. [16] and this process involves the production through the agency of anion intermediates. It was observed in their study on MgO that the superoxide ion exhibits an axial g-tensor with principal values $g_{\|}=2.070$ and $g_{\perp}=2.008$. Considerable g-anisotropy has been exhibited by O_2^- ions in systems like zeolites and metal oxides [17–19]. It was observed that the $g_{\|}$ value for the O_2^- ion was highly matrix dependent and ranged between 2.015 and 2.080 and is controlled by the magnitude of the crystal-field from the cations. $g_{\perp}$, on the other hand, is expected to be relatively close to free-electron value. Based on these findings, center I with a relatively large anisotropy in *g*-values in the present garnet system is tentatively assigned to an O_2^- ion.

Center II in Fig. 3 is due to a species characterized by a single ESR line with an isotropic *g*-value equal to 1.9995 and 5 gauss linewidth. Electrons may get trapped at oxygen ion vacancies during irradiation leading to the formation of F^+ centers. In an alkali halide system like LiF [20], the F center (an electron trapped at the F^- ion vacancy) exhibited an unusually large linewidth of about 100 gauss and a *g*-value close to the free- spin value. In contrast to LiF, F^+ center has a linewidth of about 1 gauss in MgO system [21] and this linewidth is the inherent linewidth of the center. The linewidth is determined by the ions present in a system (whether they have nuclei with magnetic moment and their abundance) and more importantly on the delocalization of the unpaired electron which depends on the host lattice. In alkali halides, the unpaired electron is considerably delocalized and interacts with several alkali and halide ions from successive neighboring shells. For example, the observed linewidth in KCl is around 20 gauss [22] and in LiCl it is 58 gauss [22]. Apart from alkali halides, centers with an electron trapped at an anion vacancy (i.e., F^+ centers) have also been observed in oxide systems. In all these systems, *g*-values are found to be close the free-electron value with a g-shift which may be positive or negative. An example of a recent observation of such a center is in pure and defective TiO_2 nanoparticles [23]. In the present case of center II, linewidth is not large and the g-shift is small. Based on these observations, center II is tentatively assigned to an F^+-center. Fig. 4 shows the thermal annealing behavior of center II. It is observed that the intensity of the ESR line associated with this center decreases in the temperature range from about 120 °C to around 260 °C. This decay appears to relate to the TL peak at 190 °C.

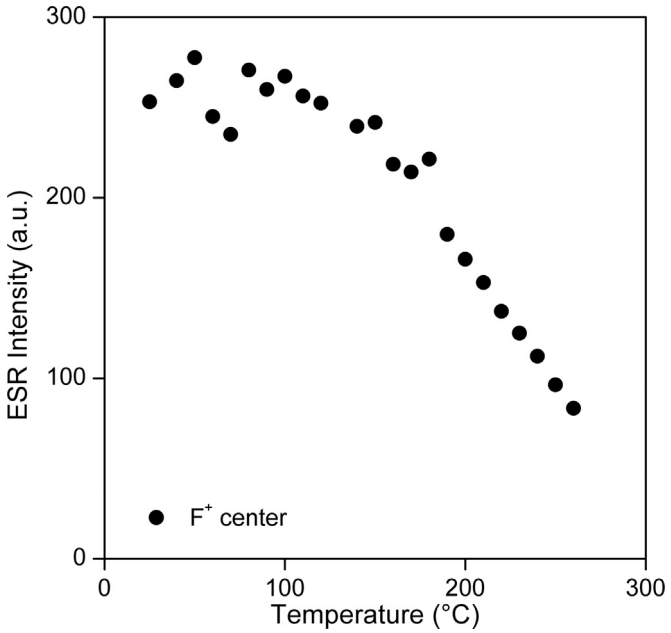

Fig. 4. Thermal annealing behavior of center II in the G7 mineral.

Why the solid solution G3, G5, G6 and G7 have such different behavior concerning their ESR spectra, is something not yet understood. After all of them belong to a same Garnet Group with a same crystal structure. Above all it is clear that the ESR properties in each sample depend upon iron-ion, particularly in (3+) state, however, in each case, in natural state this iron behaves in different way. In G3 a very strong dipole–dipole interaction takes place and the signal at $g=2.0$ is due to a very high microwave power absorption. In G5 iron (3+)-ion form magnetite molecule, in G6 large fraction of iron is in (2+) state and G7 the ESR spectrum exhibits signals at $g=4.3$ and 7.9. Much must be done to clarify all these results.

Garnets are silicate crystals with a behavior sui-generis. In nature rarely are found in a pure garnet, but the majority of them is found as solid solution of garnets belonging to a subgroup called pyralspite.

In five solid solution here studied named G3 (largest components are almandine and spessartine), G4 (almost pure almandine with small percentage of pyrope), G5 (80% of almandine and 12% pyrope), G6 similar to G4, G7 with 65% almandine and 24% pyrope, quite distinct behavior with respect to their EPR properties have been found. In G3 the spectrum consisted of a straight line in 1000 to 6000 Gauss magnetic field with an elevated slope, in G5 the natural sample presented a spectrum having a signal with $g=9.0$, in G6 no signal was found and in G7 a signal with $g=6.0$ have been observed. Why such varieties of behavior. In G5, an annealing at 800 °C the $g=9.0$ moved to 6.0 at 900 °C to 3.2. In G6 a large fraction of iron was found in (2+) state, therefore its EPR spectrum did not present practically no signal.

One common behavior is that for very high temperature annealing (900–1000 °C) all irons in the samples become individual ions and all of them presented dipole–dipole interaction.

The behavior of G5 with heat treatment indicates that in natural state large fraction of iron form Fe_3O_4 molecules, with 800 °C annealing it charge to Fe_2O_3 molecules.

No explanation was found; it is necessary to further experiments to understand such interesting properties.

4. Conclusions

ESR technique was utilized to study the evolution with temperature of paramagnetic Fe^{3+} ions and their distribution in a garnet solid solution. The formation of Fe^{3+} ions at different annealing temperatures show that $Fe^{2+} \rightarrow Fe^{3+}$ oxidation process plays an important role in the evolution of the ion. At low annealing temperatures, dipolar interactions are prevalent even at low concentrations of Fe^{3+} ions while at high temperatures, exchange interactions appear to prevail. The structure of almandine with Fe^{2+}–O–Fe^{2+} linkages facilitates such interactions. The results also indicate the clustering tendency of Fe^{3+} ions in the garnet solid solution. A broad TL peak at 190 °C is observed in the gamma irradiated garnet system. Two defect centers have been identified in the irradiated system and these are tentatively assigned to an O_2^- ion and F^+ center. The F^+ center is found to correlate with the TL peak at 190 °C.

Acknowledgments

The authors wish to thank Ms. E. Somessari and Mr. C. Gaia, Instituto de Pesquisas Energeticas e Nucleares (IPEN), Brazil, for kindly carrying out the irradiation of the samples. To FAPESP (Process number 2014/03085-0) for partial financial support and to CAPES (Process number BEX-9612130) for fellowship to T.K. Gundu Rao.

References

[1] W.A. Deer, R.A. Howie, J. Zussman, An Introduction to Rock Forming Minerals, 2nd ed., E. Prencice Hall, New York (1992), p. 391.
[2] S. Watanabe, S.R.Q. Espinoza, J.F.D. Chubaci, N.F. Cano, D.R. Cornejo, IOP Conference Series: Matererial Science and Engineering, 80, 2015, 012014-012014-4.
[3] L.P. Neves, A.P. Marques, T.K. Gundu Rao, N.N. Lucas, K.M. Sato, S. Watanabe, Optical absorption and EPR behaviors of two pyralspite garnets in solid solution, in: Proceedings of the XIII Meeting of Brazilian Society Materials Researches, João Pessoa, Pb, Brazil, 2014.
[4] M. Ikeya, New Applications of Electron Spin Resonance, World Scientific Publishing Co, Cingapura (1993), p. 279.
[5] U. Kaufmann, Phys. Rev. B 14 (1976) 1848.
[6] T. Costner, G.S. Newell, W.C. Holton, C.P. Slichter, J. Chem. Phys. 32 (1960) 668.
[7] C.M. Brodbeck, J. Non-Cryst. Solids 40 (1980) 305.
[8] G. Kitis, J.M. Gomez-Ros, W.N. Tuyn, J. Phys. D: Appl. Phys. 31 (1998) 2636.
[9] C. Geiger, Th Armbruster, G. Lager, K. Jiang, W. Lottermoser, G. Amthauer, Phys. Chem. Minerals 19 (1992) 121.
[10] G.A. Novak, G.V. Gibbs, Am. Mineral. 56 (1971) 791.
[11] M.M. Kuklja, J. Phys. Condens. Matter 12 (2000) 2953.
[12] A.P. Patel, M.R. Levy, R.W. Grimes, R.M. Gaume, R.S. Frigelson, K.J. McClellan, C. R. Stanek, Appl. Phys. Lett. 93 (2008) 191902.
[13] J. Dong, K. Lu, Phys. Rev. 43 (1991) 8808.
[14] D. Truong, M.K. Devaraju, T. Tomai, I. Honma, ACS Appl. Mater. Interfaces 5 (2013) 9926.
[15] M.S. Holston, J.W. McClory, N.C. Giles, L.E. Halliburton, J. Lumin. 160 (2015) 43.
[16] E. Garrone, A. Zecchina, F.S. Stone, J. Catal. 62 (1980) 396.
[17] D.D. Eley, M.A. Zammitt, J. Catal. 21 (1971) 366.
[18] K.M. Wong, J.H. Lunsford, J. Phys. Chem. 74 (1971) 1165.
[19] J.H. Lunsford, Catal. Rev. 8 (1973) 135.
[20] C.A. Hutchison, Phys. Rev. 75 (1949) 1769.
[21] J.E. Wertz, P. Auzins, R.A. Weeks, R.H. Silsbee, Phys. Rev. 107 (1957) 1535.
[22] W.C. Holton, H. Blum, Phys. Rev. 125 (1962) 89.
[23] B. Choudhury, A. Choudhury, Sci. Adv. Mater. 6 (2014) 2115.